Ionospheric disturbance dynamo associated to a coronal hole: Case study of 5-10 April 2010

Ibrahim Fathy, Christine Amory-Mazaudier, A. Fathy, A. M. Mahrous, K. Yumoto, E. Ghamry

AGU PUBLICATIONS

JGR

Journal of Geophysical Research: Space Physics

RESEARCH ARTICLE
10.1002/2013JA019510

Key Points:
- Planetary signature of disturbance dynamo
- Extraction of disturbance dynamo
- Period of the disturbance dynamo

Correspondence to:
C. Amory-Mazaudier,
christine.amory@lpp.polytechnique.fr

Citation:
Fathy, I., C. Amory-Mazaudier, A. Fathy, A. M. Mahrous, K. Yumoto, and E. Ghamry (2014), Ionospheric disturbance dynamo associated to a coronal hole: Case study of 5–10 April 2010, *J. Geophys. Res. Space Physics*, *119*, 4120–4133, doi:10.1002/2013JA019510.

Received 3 OCT 2013
Accepted 25 APR 2014
Accepted article online 30 APR 2014
Published online 28 MAY 2014

Ionospheric disturbance dynamo associated to a coronal hole: Case study of 5–10 April 2010

I. Fathy[1,2], C. Amory-Mazaudier[2], A. Fathy[1,3], A. M. Mahrous[1], K. Yumoto[4], and E. Ghamry[5,6]

[1]Space Weather Monitoring Center, Faculty of Science, Helwan University, Helwan, Egypt, [2]LPP/CNRS/UPMC, Saint-Maur-des-Fossés, France, [3]Physics Department, Fayoum University, Al Fayoum, Egypt, [4]International Center for Space Weather Science and Education, Kyushu University, Fukuoka, Japan, [5]National Research Institute of Astronomy and Geophysics, Helwan, Cairo, Egypt, [6]School of Space Research, Kyung Hee University, Yongin, South Korea

Abstract In this paper we study the planetary magnetic disturbance during the magnetic storm occurring on 5 April 2010 associated with high-speed solar wind stream due to a coronal hole following a coronal mass ejection. We separate the magnetic disturbance associated to the ionospheric disturbance dynamo (Ddyn) from the magnetic disturbance associated to the prompt penetration of magnetospheric electric field (DP2). This event exhibits different responses of ionospheric disturbance dynamo in the different longitude sectors (European-African, Asian, and American). The strongest effect is observed in the European-African sector. The Ddyn disturbance reduces the amplitude of the daytime *H* component at low latitudes during four consecutive days in agreement with the Blanc and Richmond's model of ionospheric disturbance dynamo. The amplitude of Ddyn decreased with time during the 4 days. We discuss its diverse worldwide effects. The observed signature of magnetic disturbance process in specific longitude sector is strongly dependent on which Earth's side faces the magnetic storms (i.e., there is a different response depending on which longitude sector is at noon when the SSC hits). Finally, we determined an average period of 22 h for Ddyn using wavelet analysis.

1. Introduction

The geomagnetic storm of 5 April 2010 was studied at low latitudes using magnetic and ionospheric data sets in Egypt by *Shimeis et al.* [2012]. This event was previously studied by *Möstl et al.* [2010] who described in detail the shock associated with the coronal mass ejection of 3 April 2010 and by *Connors et al.* [2011] who analyzed the magnetic flux transfer event associated with the impact of the shock on the magnetosphere on 5 April 2010 at 08:25 UT. The present study is a continuation of the last mentioned work as we still need more morphological analysis of the ionospheric disturbance dynamo process.

The novelty of this study is the analysis at the planetary scale of the geomagnetic disturbance associated with this event using ground magnetometers along European-African, Asian, and American sector. We propose a method to isolate the part of the geomagnetic disturbance due to the ionospheric disturbance dynamo process [*Blanc and Richmond*, 1980]. The geomagnetic disturbances observed at ground level are the sum of magnetic disturbances related to the different current systems flowing in the magnetosphere and ionosphere [*Cole*, 1966; *Fukushima and Kamide*, 1993]. At low latitudes the geomagnetic disturbance related to ionospheric electric currents is mainly due to the intensification of the auroral electrojets. Two main physical processes cause large-scale ionospheric current systems connecting high and low latitudes: (1) the direct prompt penetration of the magnetospheric convection electric field [*Vasyliunas*, 1970] and (2) the ionospheric disturbance dynamo [*Blanc and Richmond*, 1980]. The direct prompt penetration of magnetospheric convection affects simultaneously high and low latitudes and was interpreted by *Nishida et al.* [1966] as the transmission of the magnetospheric convection electric field from high to low latitudes. The magnetic disturbance associated to this physical process was named DP2 current system by *Nishida* [1968]. *Blanc and Richmond* [1980] proposed the physical process of the ionospheric disturbance dynamo to interpret the delayed effects of storms. *Le Huy and Amory-Mazaudier* [2005, 2008] isolated the magnetic disturbance due to this physical process and named it disturbance dynamo (Ddyn). They isolated this Ddyn disturbance only on very specific days just after a storm related to a single coronal mass ejection (CME). On these specific days, there is no DP2 current system associated to the prompt penetration of magnetospheric convection, and therefore, it was possible to study the sole magnetic signature of Ddyn.

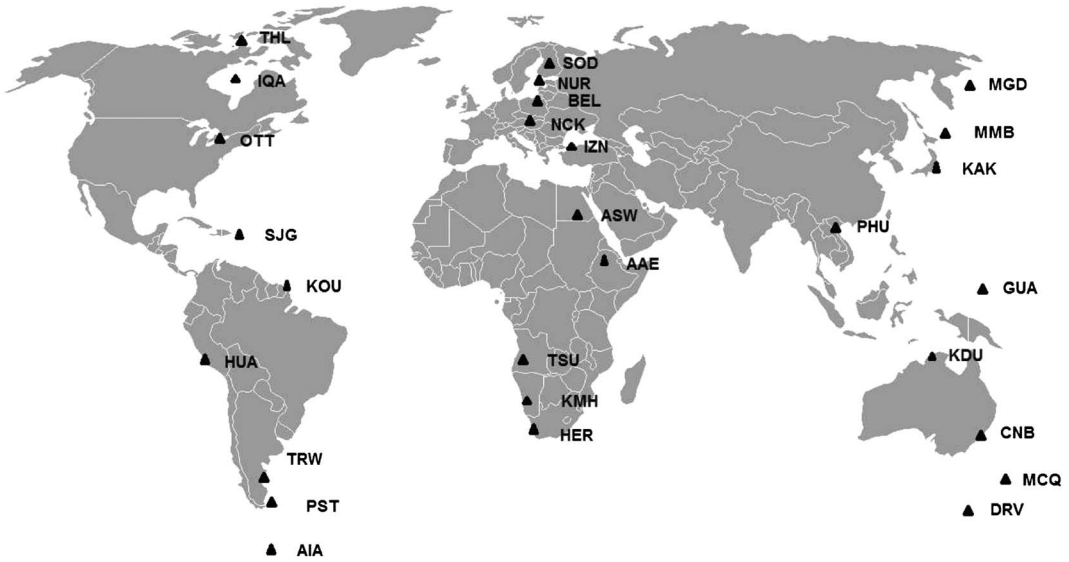

Figure 1. Planetary map of the 28 magnetic observatories (27 INTERMAGNET networks and 1 MAGDAS network).

During the last decades experimental and theoretical studies illustrated the characteristics of the ionospheric disturbance dynamo [*Fejer et al.*, 1983; *Mazaudier and Venkateswaran*, 1990; *Richmond et al.*, 2003; *Zaka et al.*, 2010; *Huang*, 2013]. The main characteristic of the magnetic signature associated with the ionospheric disturbance dynamo (Ddyn) observed on magnetic data [*Mayaud*, 1982; *Fambitakoye et al.*, 1990; *Le Huy and Amory-Mazaudier*, 2005] is a decrease of the amplitude of the *H* component at the magnetic equator. This decrease is due to a disturbed westward equatorial electrojet flow opposite to the regular eastward equatorial electrojet flow. The latitudinal profile of the Ddyn disturbance dynamo magnetic signature exhibits an eastward current at middle latitudes and a westward one at low latitudes with a substantial amplification at the magnetic equator. Such current flow reveals an "anti-*Sq*" system established between the middle latitudes and the equatorial region and opposes the normal *Sq* current vortex. However, the localization of the eastward current and consequently the position and the extent of the anti-*Sq* current vortex changing depend on strength of the storm [*Le Huy and Amory-Mazaudier*, 2005]. The latitudinal profile of the Ddyn disturbance and the disturbance DP2 generated by the mechanism of prompt penetration of the magnetospheric convection electric field shows, in general, a weak disturbance at the low latitudes with a substantial amplification at the magnetic equator. *Zaka et al.* [2009] found that depending on the intensity of the storm, the magnitude of the DP2 appears higher than the Ddyn over the American and Asian sector contrary to the African sector.

In this paper we perform a detailed study of the case of 5–10 April 2010 with planetary magnetic signature of high-speed solar wind streams due to coronal hole using 28 magnetometers all over the world along three longitude sectors (African-European, Asian, and American) to see more morphological effects of ionospheric disturbance dynamo process on magnetic data on the global scale. Section 2 describes the data and data processing that show the main morphological characteristics of the storm event and proposes a method to isolate the Ddyn magnetic disturbance. Section 3 presents the data analysis, and section 4 data interpretation. Section 5 is devoted to the discussion and the conclusion.

2. Data Set and Data Processing

We analyzed the whole period from 3 to 10 April which included magnetic quiet period followed by a storm (which was discussed by *Shimeis et al.* [2012]) using ground (Aswan MAGDAS station), ionospheric (Helwan GPS SCINDA), and satellite (solar wind parameters) data to study the ionospheric signature of high-speed solar wind streams on 6–8 April 2010 following a storm driven by a CME on 5 April 2010.

In the present work we continue on the same event but with planetary magnetic effects using International Real-time Magnetic Observatory Network (INTERMAGNET) magnetometers network along three longitudinal sectors: African-European, Asian, and American. Figure 1 shows the world planetary map of 28 magnetic

Table 1. Geographic and Geomagnetic Coordinates of Magnetic Observatories

		Geographic		Geomagnetic	
Code	Name	Latitude	Longitude	Latitude	Longitude
AAE	Addis Ababa	9.02	38.77	5.3	111.8
AIA	Akademic Vernadsky	−65.25	295.75	−55.0	5.5
ASW	Aswan	23.59	32.51	15.20	104.24
BEL	Belsk	51.84	20.79	50.2	105.2
CNB	Canberra	−35.32	149.36	−42.7	226.9
DRV	Dumont d'Urville	−66.37	140.01	−74.5	231.2
GUA	Guam	13.59	144.87	5.3	215.7
HER	Hermanus	−34.43	19.23	−34.0	84.0
HUA	Huancayo	−12.05	284.67	−1.8	356.5
IQA	Iqaluit	63.75	−68.52	74.0	5.2
IZN	Iznik	40.50	29.73	37.7	109.6
KAK	Kakioka	36.23	140.18	27.4	208.8
KDU	KAKADU	−12.69	132.47	−22.0	205.6
KMH	Keetmanshoop	−26.54	18.11	−36.64	84.35
KOU	Kourou	5.10	−52.70	11.9	19.5
MCQ	Macquarie	−54.50	158.95	−60.1	244.3
MGD	Magadan	60.05	150.73	52.3	213.9
MMB	Memembetsu	43.90	144.20	35.4	211.3
NCK	Nagycenk	47.63	16.72	46.9	99.6
NUR	Nurmijarvi	57.70	24.70	55.9	113.2
OTT	Ottawa	45.40	−75.55	55.6	355.3
PHU	Phuthuy	21.03	105.95	10.8	177.9
PST	Port Stanley	−51.70	302.11	−41.7	11.5
SJG	San Juan	18.11	−66.15	28.6	6.1
SOD	Sodankyla	67.37	26.63	63.9	120.0
THL	Thule	77.47	−69.23	87.7	14.1
TRW	Trelew	−43.26	−65.38	−33.1	5.6
TSU	Tsumeb	−19.20	17.58	−18.8	85.9

observatories. Table 1 gives the codes, name, geographic, and geomagnetic coordinates of the 28 ground stations (27 INTERMAGNET stations and 1 MAGDAS station).

The horizontal Earth's magnetic component (H) is computed from the north component of the magnetic field (X) and the east component of the magnetic field (Y) by using the following simple expression for most of the INTERMAGNET stations.

$$H = \sqrt{X^2 + Y^2} \tag{1}$$

We use the solar wind parameters *Vx* and interplanetary magnetic field (IMF) *Bz* recorded on board the ACE satellite (http://www.srl.caltech.edu/ACE/ASC/browse/view_browse_data.html), the magnetic indices *Dst*, *AU*, and *AL* that are from Data Analysis Center for Geomagnetism and Space Magnetic Graduate School of Science, Kyoto University website (http://wdc.kugi.kyoto-u.ac.jp/wdc/Sec3.html), and the *Am* magnetic indices (http://isgi.cetp.ipsl.fr).

The magnetic indices *Dst*, *AU*, and *AL* give estimation of the magnetospheric and auroral electric currents. The *Am* magnetic indices allow the selection of magnetic quiet days [*Mayaud*, 1980; *Menvielle and Marchaudon*, 2008]. The criterion for the selection of a magnetic quiet day is that the daily average *Am* index is smaller than 20 nT. Table 2 gives the value of the *Am* index for the analyzed period, and Table 3 gives the *Am* values of the quietest days of April.

The mean averaged *H* component is computed by the mean arithmetical value of the *H* component of magnetic quiet days. To evaluate the mean regular variation of the S_R, we used the quietest days of the

Table 2. Daily Values of the *Am* Index From 3 to 10 April 2010

Quiet Days	3 April	4 April	5 April	6 April	7 April	8 April	10 April
Daily $<Am>$	16 quiet	25	64	60	38	21	5 quiet

Table 3. List of the Most Magnetic Quiet Days of April 2010 Determined With the *Am* Indices

Quiet Days	13 April	16 April	18 April	25 April	26 April	28 April	30 April
Daily $<Am>$	4	4	2	3	2	4	4

month with the daily $Am < 20$ nT. They are listed in Table 3. In order to understand the ionospheric electric current disturbance (D_{iono}) we need to extract from the observed H the effect of the magnetospheric current and the regular current S_R.

The ionospheric disturbance (D_{iono}) is given by the following relations [*Shimeis et al.*, 2012]

$$D_{\text{iono}} = H - Dst \cdot \cos(\lambda) - S_R \tag{2a}$$

$$D_{\text{iono}} = \text{DP2} + \text{Ddyn} \tag{2b}$$

where λ is the colatitude of the station.

To separate the effect of the DP2 signal from the disturbance dynamo (Ddyn) signal, we take the average value of 4 h with sliding of 1 h for the whole period of study for ASW, PHU, and SJG stations by using some MATLAB programs (interpolation, average, and mean).

3. Data Analysis

Figure 2 is composed of four panels illustrating the following: (a) the time variation of the *Vx* component solar wind speed with resolution of 1 min *Vx* (km/s), (b) the *z* component of the interplanetary magnetic field with a resolution 5 min, *Bz* (nT), (c) the *Dst* magnetic index in nanotesla, and (d) the *AU* (nT) and *AL* (nT) indices with time resolution of 1 min. The variation of solar wind parameters and geomagnetic indices is given in Table 4 for the whole period.

On 5 April 2010 *Vx* increased from 498 to 800 km/s at the time of the storm sudden commencement SSC (08:25 UT) and reached the maximum value at 13:00 UT. It remained at 600 km/s (on average) from 6 to 8 April 2010. *Vx* started to decrease around 18:00 UT on 8 April 2010, to reach 450 km/s on 9 April 2010

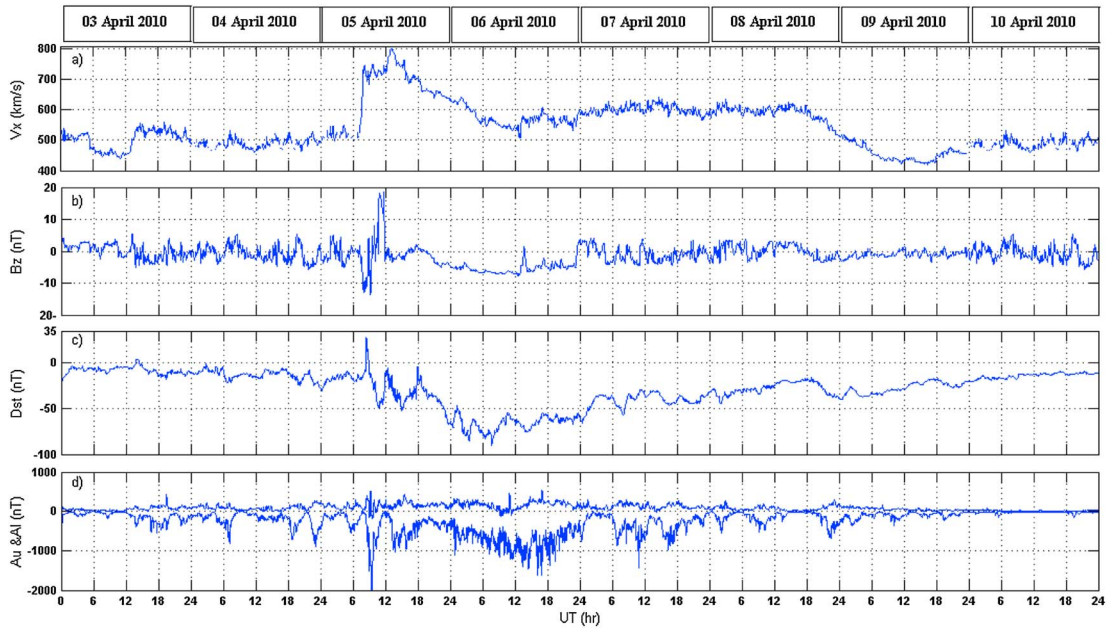

Figure 2. The solar wind parameters and geomagnetic indices for high-speed streams from 3 to 10 April 2010: (a) component *Vx* of the solar wind speed, (b) the *Bz* component of the interplanetary magnetic field, (c) the *Dst* index, and (d) the *AU* and *AL* indices.

Table 4. Solar Wind Parameters and Geomagnetic Indices From Minimum to Maximum Values for the Whole Period

Day	*Vx* (km/s)	*Bz* (nT)	*Dst* (nT)	*AL* (nT)
3 April	444 to 559	−4.9 to 5.5	−22 to 4	−467
4 April	460 to 533	−5.8 to 6	−28 to −1	−836
5 April	498 to 800	−12.3 to 18.86	−67 to 28	−2104
6 April	507 to 642	−7.6 to 2.6	−90 to −47	−1610
7 April	567 to 642	−4.4 to 4.1	−66 to −29	−1493
8 April	518 to 632	−3.8 to 3.7	−45 to −16	−675
9 April	420 to 520	−3.3 to 1.5	−40 to −17	−369
10 April	345 to 460	−2.11 to 3.3	−21 to −9	−158

around 12:00 UT, and increased again until 500 km/s at about 00:00 UT on 10 April 2010. The IMF *Bz* turned southward at around 08:25 UT on 5 April 2010 and reached the maximum value of −19 nT. It remained negative for several hours until 10:30 UT on 5 April 2010, except for several northward excursions until 11:00 UT on April 2010. IMF *Bz* turned southward again around 11:00 UT and remained negative 1 day on 6 April 2010, except where it exhibits a northward peak. IMF *Bz* returned to its values before the storm at 03:00 UT on 7 April 2010. The *Dst* increased strongly from −10 nT to 35 nT at the time of SSC. Then it decreased and had two negative peak excursions of the same amplitude −50 nT around 11:00 UT and 14:00 UT during the main phase of the storm on 5 April 2010. The *Dst* reached the minimum value of −90 nT around 12:00 UT on 6 April 2010. *Dst* returned to its values before the storm on 10 April 2010, around 03:00 UT. *AU* and *AL* indices exhibited three main maximum values on 5 April 2010 around 08:26 UT (350 nT for *AU* and −2104 nT for *AL*), on 6 April 2010 around 01:26 UT (350 nT for *AU* and −1610 nT for *AL*), and on 7 April 2010 around 17:30 UT (350 nT for *AU* and −1493 nT for *AL*). At the SSC time, the increase of *Vx* from 500 to 800 km/s is associated with an increase of the southward IMF *Bz* component 19 nT and *Dst* and *AL* and *AU* amplitude increases. All these observations are the effects of the shock associated with the coronal mass ejection of 3 April 2010 which reaches the Earth on 5 April 2010 [*Möstl et al.*, 2010] followed by high-speed solar wind streams related to coronal hole. Figure 3 shows the variation (*x* axis) of the *H* component for all the stations of the European-African sector from 3 to 10 April 2010 (*y* axis). At the time of the SSC, all the stations exhibit the signature of the prompt penetration of the convection electric field. Before the storm and several days after the storm we can observe for each station the regular variation of the Earth's magnetic field S_R. The S_R of *H* is positive at stations between the equator and the focus of the *Sq* current system in both hemispheres (AAE, ASW, and IZN). The S_R of *H* is negative at stations between the focus of *Sq* and the pole for both hemispheres (NUR and HER). These observations correspond to the well-known *Sq* pattern composed of two cells, one in each hemisphere. This figure highlights also that the return to the regular variations does not occur on the same day in all the stations; it occurs at Adis Ababa 1 day before Aswan. Similar figures made for the American and Asian sectors show the same features.

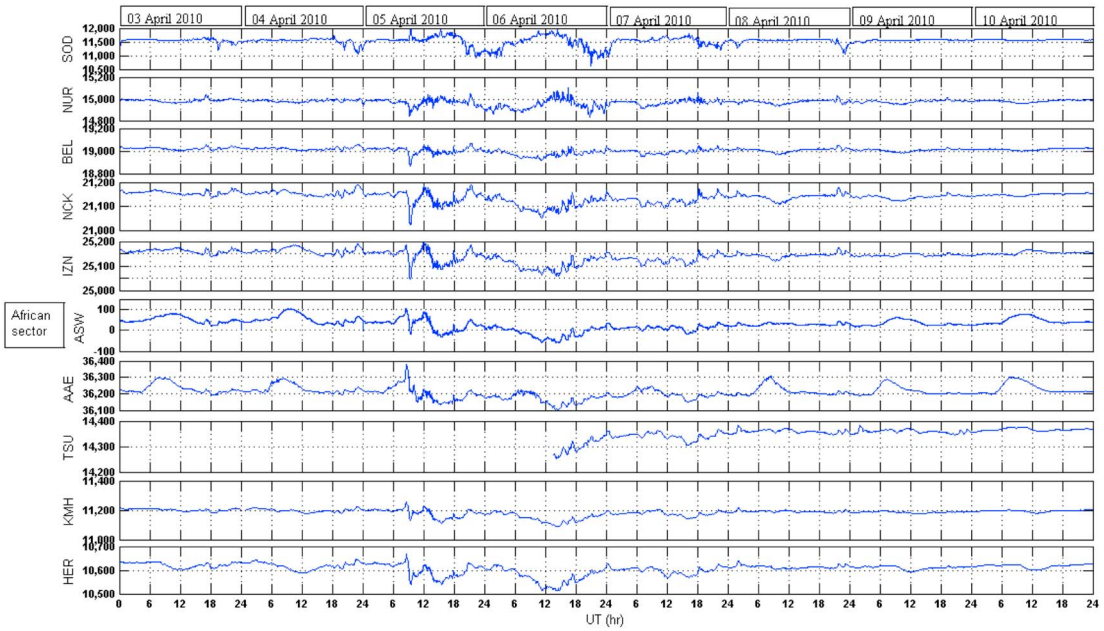

Figure 3. The African stations from high latitudes to equatorial latitudes for the two hemispheres from 3 to 10 April 2010.

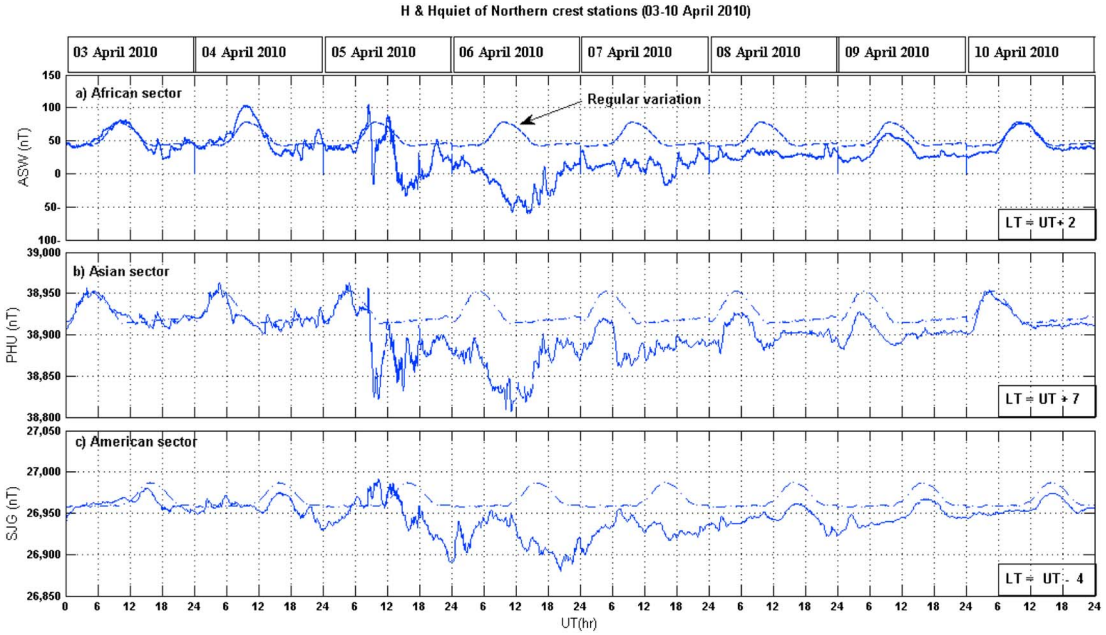

Figure 4. Superposition of regular variation (computed for the magnetic quiet days of *H* components) as dashed curve and the raw data for three stations in (a) African, (b) Asian, and (c) American sectors with local time for each station at northern crest latitude plotted with universal time from 3 to 10 April 2010.

Figures 4–6 are compose of three panels where the *H* component (solid line) is superimposed on the *H* quiet (dashed line) plotted with universal for Northern Hemisphere, equatorial, and Southern Hemisphere for each African-European, Asian, and American sectors, respectively, with the local time offset from UT given for each station.

In Figures 4a–4c the *H* component of the Earth's magnetic field measured at ASW, PHU, and SJG (solid line) is superimposed on the quiet reference level *H* quiet (dashed line). The dashed line exhibit the well-known

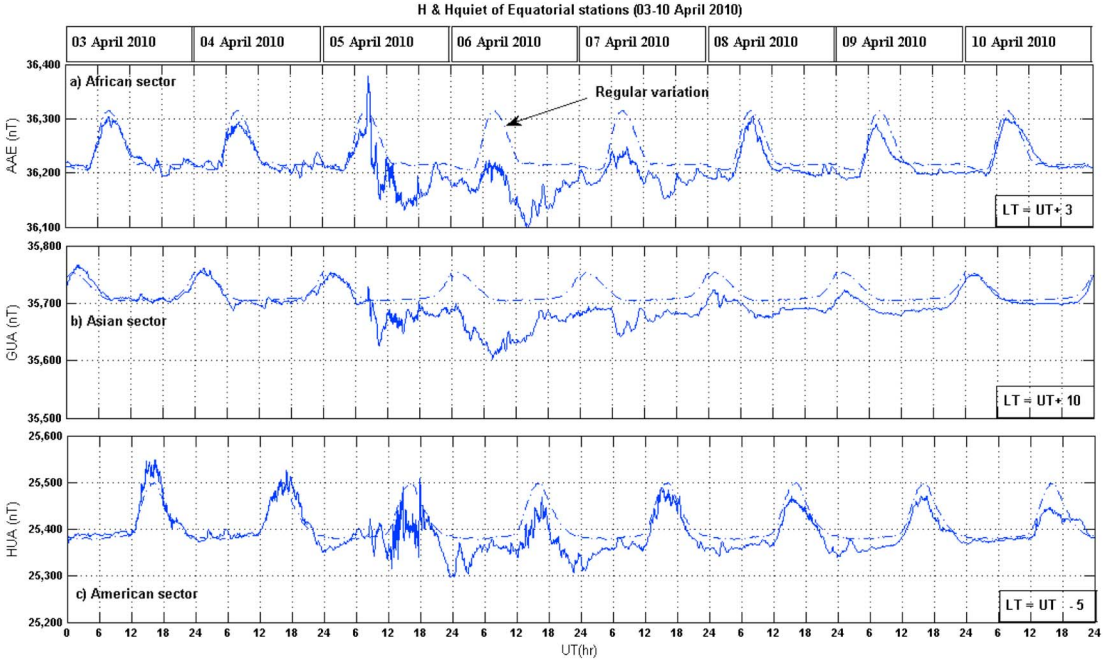

Figure 5. Superposition of regular variation (computed for the magnetic quiet days of *H* components) as dashed curve and the raw data for three stations in (a) African, (b) Asian, and (c) American sectors with local time for each station at equatorial latitude plotted with universal time from 3 to 10 April 2010.

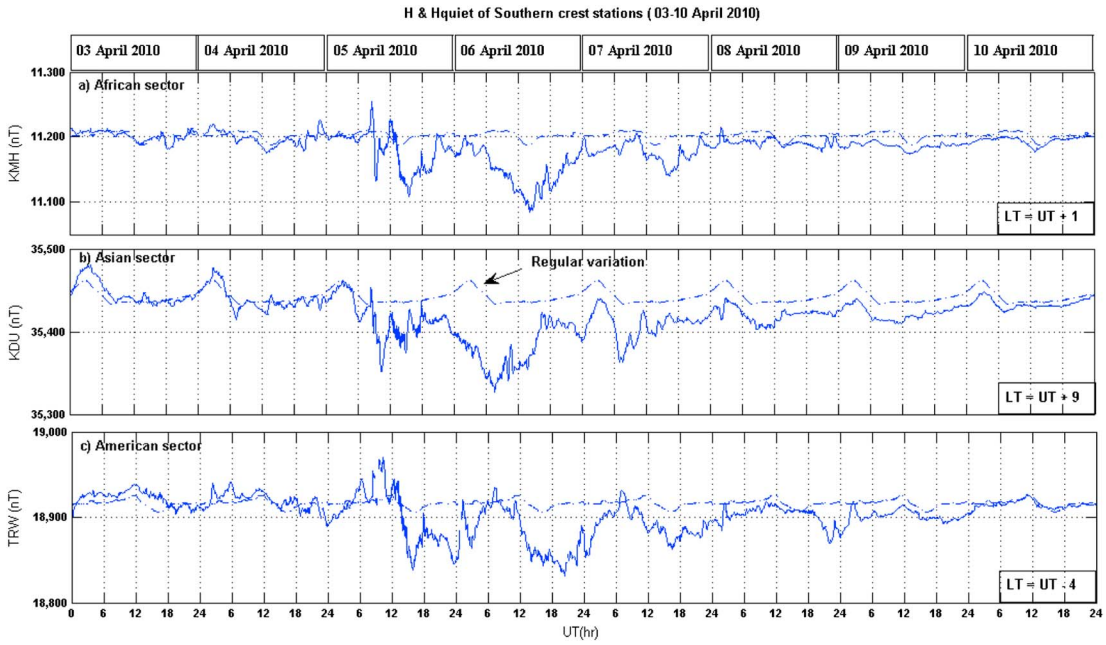

Figure 6. Superposition of regular variation (computed for the magnetic quiet days of *H* components) as dashed curve and the raw data for three stations in (a) African, (b) Asian, and (c) American sectors with local time for each station at southern crest latitude plotted with universal time from 3 to 10 April 2010.

regular pattern of *Sq* for stations located below the focus latitude in the Northern Hemisphere. We must recall here that we used the raw data of the MAGDAS network. The MAGDAS network gives the relative variation of the *H* component and not the absolute value as the INTERMAGNET network. Figure 4a shows a value of 50 nT during night. This value represents the zero level of the regular variation *Sq*, as we know that there is no *Sq* currents on the nightside due to the weakness of the conductivities. As a consequence the real *H*-ASW is around 30 nT if we cut the midnight zero level around 50 nT. In the following we will use the raw data of MAGDAS. On April 2010, the day before the storm the *H*-ASW is higher than the *H* quiet about 30 nT. We can observe the typical *H* with *H* quiet for ASW and PHU of days 3 and 10 which are different for SJG. We must recall here that the amplitude of the *H* component depends on the latitude of the station. We can observe the effects of the storm on 5–7 April, for the three stations, with high fluctuations on 5 April at ASW and PHU stations and smaller ones at SJG. On 6 April largest disturbances in direction anti-*Sq* are observed for the three stations and then smaller fluctuations for the days 7–9 to reach the most quiet day on 10 April, except for SJG station with about 15 nT difference. For each station we have marked the local time relation with universal time.

In Figures 5a–5c the *H* component of the Earth's magnetic field measured at AAE, GUA, and HUA (solid line) is superimposed on the quiet reference level *H* quiet (dashed line). The dashed line exhibit the well-known regular pattern of the *Sq* for equatorial latitude. It is clear that an enhancement in *H*-AAE at the time of the SSC (11:26 LT) by about 75 nT above the quiet time levels. This response is not seen at GUA (18:26 LT) and HUA (3:26 LT). These two stations are on the evening and night sides. The magnetic disturbance is observed on the day of the SSC/shock arrival (5 April) and the following 2 days at AAE and GUA. There are deviations from the quiet day at all stations up until 10 April.

In Figures 6a–6c the *H* component of the Earth's magnetic field measured at KMH, KDU, and TRW (solid line) is superimposed on the quiet reference level *H* quiet (dashed line). The dashed line exhibit the well-known regular pattern of the *Sq* for KMH and TRW stations located below the focus of the Southern Hemisphere and KDU station above the focus. It is clear that an enhancement in KMH and TRW at the time of the SSC by about 50 nT above the quiet time average. KDU observed a smaller enhancement 25 nT. It is clear that there are 2 days after the storm with larges fluctuations for KMH and KDU, while for TRW there are three disturbed days after the storm with a disturbance decreasing gradually. We see also the fluctuations peak at the stations appearing at the daytime from the marked local time relation. Figures 7–9 are composed of three panels illustrating the D_{iono} disturbance (equation (1)) as a function of universal time.

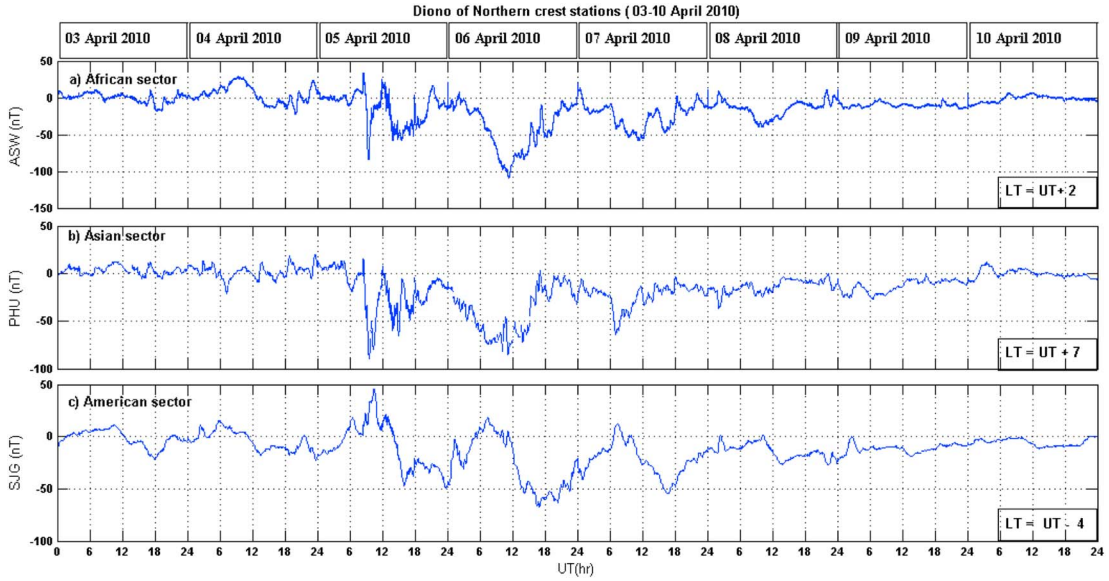

Figure 7. Ionospheric disturbances (D_{iono}) of northern crest stations for (a) African, (b) Asian, and (c) American sectors plotted with universal time from 3 to 10 April 2010.

Figures 7a–7c illustrate the daily variation of D_{iono} for ASW, PHU, and SJG stations, respectively, during the period of study. For the three stations D_{iono} exhibits an irregular pattern with different minima on the dayside. D_{iono} combines DP2 equivalent current due to the prompt penetration of the magnetospheric convection (clearly observed at the SSC of the initial phase of the storm) and the D_{dyn} equivalent current related to the ionospheric disturbance dynamo. We can note that on 5 April, the enhancement of D_{iono}-ASW 35 nT and sudden decrease to reach −77 nT, D_{iono}-PHU suddenly decreased to reach −80 nT, and D_{iono}-SJG increased to 48 nT and suddenly decreased to reach −45 nT. During the recovery phase, on 6–8 April the amplitudes of the minima of ASW station are, respectively, −110 nT, −57 nT, and −40 nT, occurring at 12:00 UT/14 LT, 12:00 UT/14 LT, and 10:00 UT/12 LT. Also, on 6–8 April for PHU station the amplitudes of the minima are, respectively, −80 nT, −65 nT, and −35 nT, occurring at 12:00 UT/19 LT,

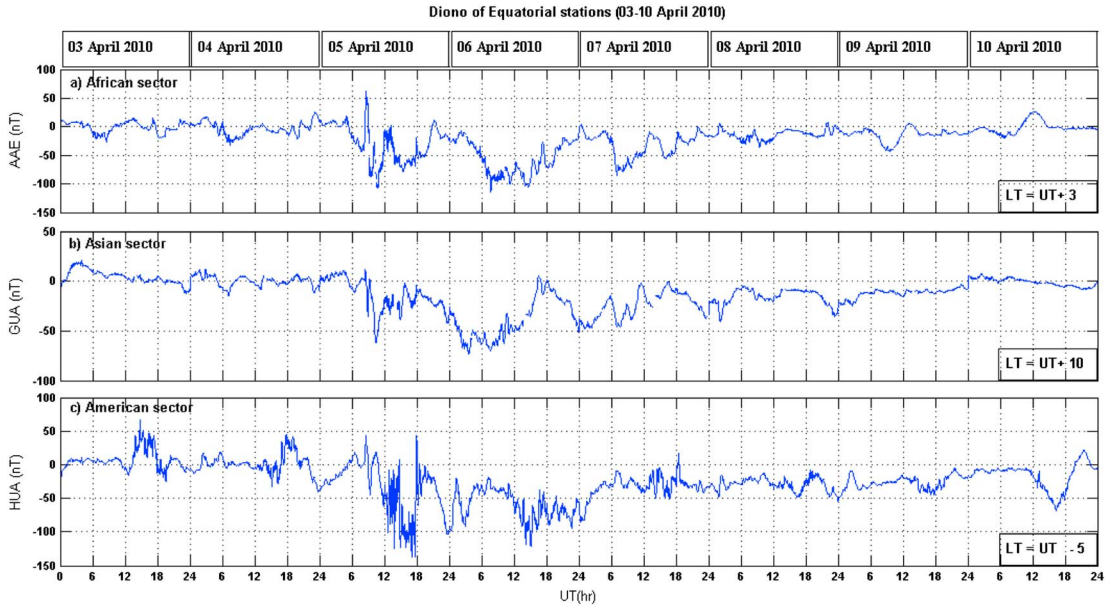

Figure 8. Ionospheric disturbances (D_{iono}) of equatorial stations for (a) African, (b) Asian, and (c) American sectors plotted with universal time from 3 to 10 April 2010.

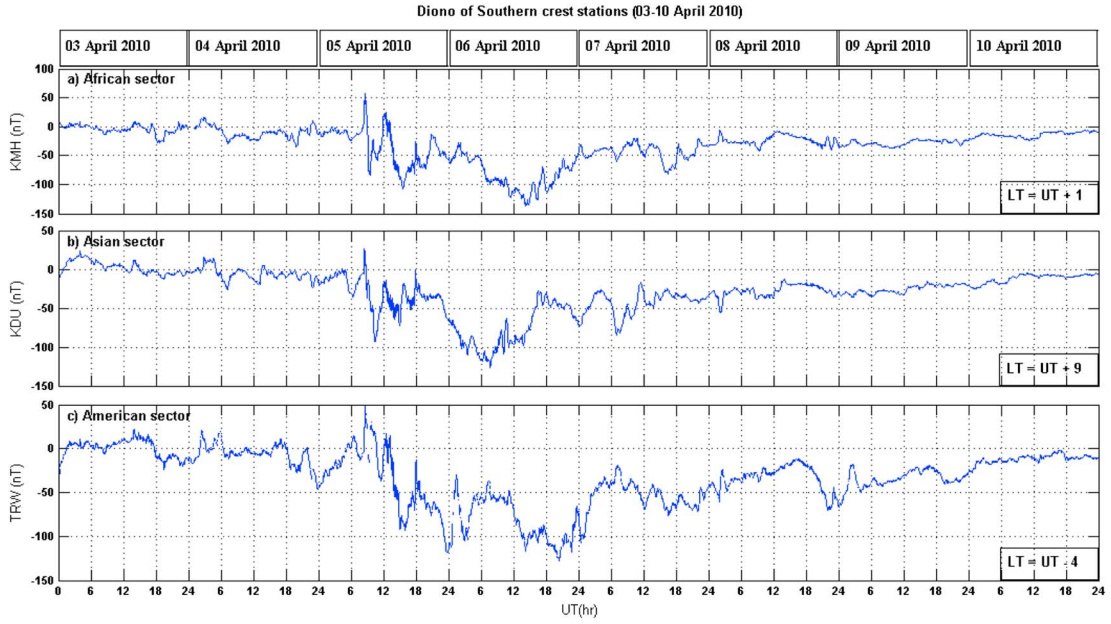

Figure 9. Ionospheric disturbances (D_{iono}) of southern crest stations for (a) African, (b) Asian, and (c) American sectors plotted with universal time from 3 to 10 April 2010.

07:00 UT/14 LT, and 02:00 UT/09 LT. For SJG station the amplitudes of the minima on 6–8 April are, respectively, −65 nT, −53 nT, and −25 nT, occurring at 18:00 UT/14 LT, 18:00 UT/14 LT, and 14:00 UT/10 LT.

Figures 8a–8c illustrate the daily variation of D_{iono} for AAE, GUA, and HUA stations, respectively, during the period of study. The three stations exhibit an irregular pattern with different minima on the dayside. The DP2 equivalent current, due to prompt penetration of magnetospheric convection, is strong especially at HUA at SSC of the initial phase of the storm. We can note that on 5 April the enhancement of the D_{iono}-AAE 65 nT suddenly decreased to reach −105 nT, D_{iono}-GUA suddenly decreased to reach −65 nT, and D_{iono}-HUA increased to 48 nT and suddenly decreased to reach −48 nT. During the recovery phase, on 6–8 April the amplitudes of the minima are, respectively, −100 nT, −80 nT, and −35 nT occurring at 12:00 UT/15 LT, 07:00 UT/10 LT, and 09:00 UT/12 LT, respectively, for the AAE station. Also, on 6–8 April the amplitudes of the minima are, respectively, −75 nT, −50 nT, and −40 nT occurring at 04:00 UT/14 LT, 24:00 UT/10 LT, and 09:00 UT/19 LT, respectively, for the GUA station. And also on 6–8 April the amplitudes of the minima are −120 nT, −50 nT, and −50 nT occurring at 15:00 UT/10 LT, 15:00 UT/10 LT, and 15:00 UT/10 LT, respectively, for the HUA station.

Figures 9a–9c illustrate the daily variation of D_{iono} at KMH, KDU, and TRW stations, respectively, during the period of study. D_{iono} for the three stations exhibits an irregular pattern with different minima on the dayside. As for Figures 7 and 8 the DP2 equivalent current due to the prompt penetration of magnetospheric convection is large during the initial phase of the storm. We can note that on 5 April the enhancement of D_{iono}-KMH 55 nT suddenly decreased to reach −79 nT, D_{iono}-KDU suddenly decreased from 30 nT to reach −90 nT, and D_{iono}-TRW increased to 40 nT and suddenly decreased to reach −40 nT. During the recovery phase on 6–8 April the amplitudes of the minima are, respectively, −130 nT, −75 nT, and −40 nT occurring at 15:00 UT/16 LT, 15:00 UT/16 LT, and 09:00 UT/10 LT, respectively, for KMH station.

For KDU, on 6–8 April, the amplitudes of the minima were, respectively, −125 nT, −80 nT, and −50 nT occurring at 08:00 UT/16 LT, 08:00 UT/16 LT, and 03:00 UT/12 LT. On 6–8 April the amplitudes of the minima at TRW are, respectively, −130 nT, −75 nT, and −75 nT occurring at 20:00 UT/16 LT, 18:00 UT/14 LT, and 22:00 UT/18 LT.

Figure 10 illustrates the superposition of mean D_{dyn} variation for ASW, PHU, and SJG stations plotted with universal time: it is clear that the three stations start and end nearly at the same time due to the effect of high-speed streams solar wind. The amplitude observed on 3, 9, and 10 April appears quiet with respect to the whole period. On these days the variability observed corresponds to the day-to-day variability of the S_R. We can note that on 5 April D_{dyn}-ASW was decreasing to −40 nT at 15:00 UT, D_{dyn}-PHU to −38 nT at 10:00 UT, and D_{dyn}-SIG was reaching 21 nT at 12:00 UT/08 LT. During the recovery phase on 6–8 April the amplitudes of the minima of

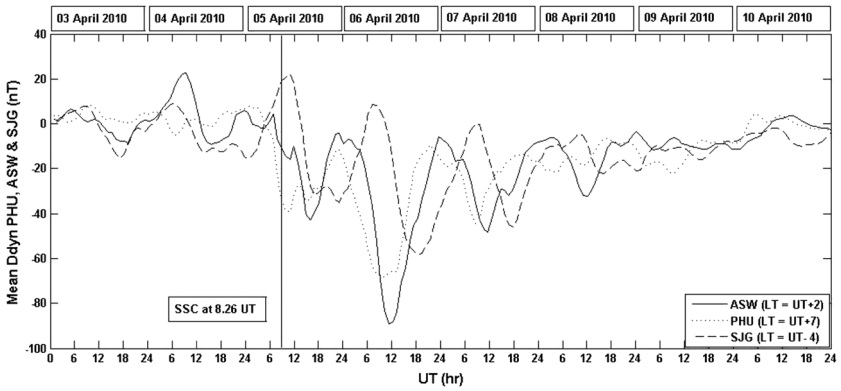

Figure 10. Superposition of the variation of ionospheric disturbance dynamo (Ddyn) computed for Aswan, Phu Thuy, and San Juan observatories from 3 to 10 April 2010.

ASW are, respectively, −90 nT, −40 nT, and −30 nT occurring at 12:00 UT for the 3 days. On 6–8 April the amplitudes at PHU are, respectively, −65 nT, −38 nT, and −20 nT occurring around 10:00 UT for the 3 days. On 6–8 April the amplitudes at SJG are, respectively, −67 nT, −51 nT, and −25 nT occurring around 16:00 UT, 16:00 UT, and 14:00 UT.

Table 5 set up together the values of the different maxima. On April 5–8, the minima occurred roughly around the same local time in each station except for ASW on the first day 5 April at PHU: 17 LT, 17 LT, 16 LT, and 19 LT; at ASW: 18 LT, 13 LT, 14 LT, and 14 LT; and at SJG: 13 LT, 14 LT, 14 LT, and 11 LT. This similar feature is also characteristic of the ionospheric disturbance dynamo which is local time dependent.

Figures 11a–11c illustrate the continuous wavelet transformation of the D_{dyn} at PHU, ASW, and SJG, respectively, of the time series signal shown in Figure 10 using Morlet base wavelet function. The *X* axis is the universal time in hours, while the vertical *Y* axis is the inverse of the frequency or the period of the signal in hours, and the rightmost column is the color index which represents the power amplitude. It is clear from the three panels that the dominant period of the D_{dyn} which is characterized by high power spectrum in the period with an average value of 22 h (approximately diurnal).

Figures 12a and 12b illustrate the cross-wavelet power spectrum of both ASW-PHU and ASW-SJG, respectively. We set ASW as a reference station to illustrate the direction of the D_{dyn}, which could be easily revealed through the relative phase shift. It is clear from Figure 12a that the direction of the arrows, which represents the relative phase, shifts between ASW and PHU in the azimuthally upward direction. According to *Grinsted et al.* [2004], the first time series of PHU station leads ASW station. It means that the direction of D_{dyn} is from PHU to ASW. Figure 12b corresponds to the stations ASW and SJG; the direction of the arrows in the downward direction means that D_{dyn} is observed first by ASW station, then by SJG.

Table 5. Time of the Maxima of Ddyn Ionospheric Disturbance Dynamo

Station	Day	Time of Maxima (UT)	Time of Maxima (LT)	Amplitude of Maxima (nT)
PHU	5 April 2010	10	17	−39
ASW		16	18	−42
SJG		17	13	−35
PHU	6 April 2010	10	17	−70
ASW		12	14	−90
SJG		18	14	−58
PHU	7 April 2010	9	16	−45
ASW		11	13	−50
SJG		18	14	−48
PHU	8 April 2010	12	19	−18
ASW		12	14	−36
SJG		15	11	−24

Wavelet transformations showed that the dominant period of the D_{dyn} is in the period 22 h. However, all the stations has this comparable period of D_{dyn}, We cannot confirm at any station the strength of the effect of the event is clearly higher that the other, but Figure 11 reveals that the event also has a comparable time interval of its effect at all stations. The cross-wavelet spectrum analysis revealed that the D_{dyn} has a direction from PHU passing by ASW then to SJG or from west to east direction.

In summary, at the beginning of the event, the observations of solar and

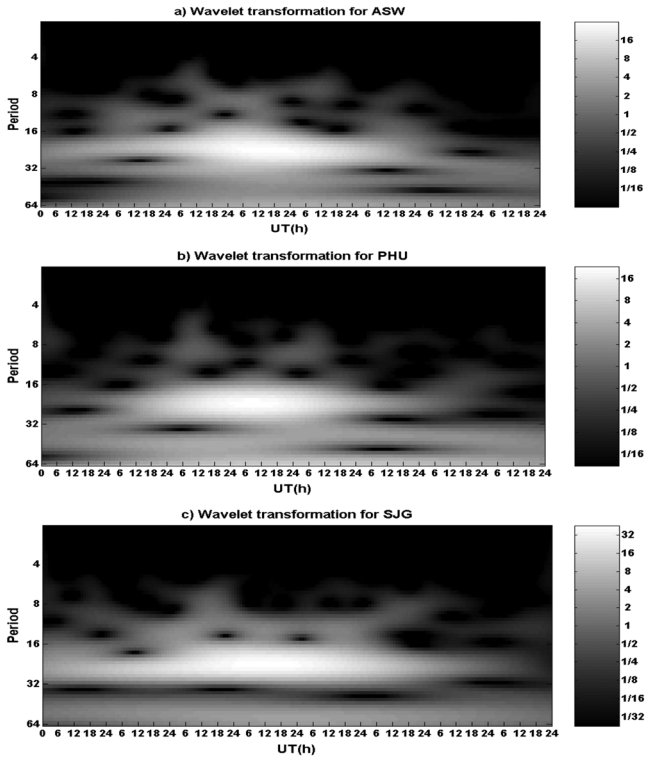

Figure 11. Illustration of the continuous wavelet transformation of (a) PHU station, (b) ASW station, and (c) SJG station. The vertical axis illustrates the period of the signal in hours, and the horizontal axis is the universal time in hours. It is clear that the dominant frequency of the signal around the period of 22 h in the time interval from 45 to 125 h, as it is clear from the color index.

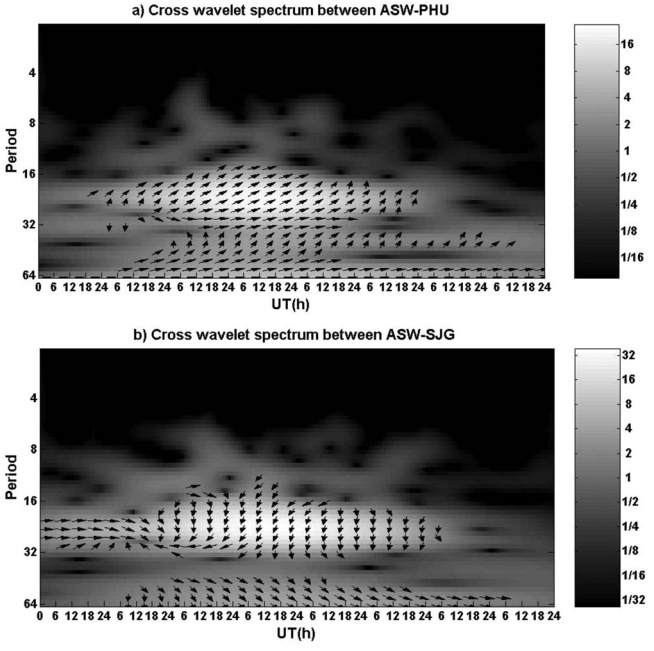

Figure 12. Cross-wavelet spectrum between (a) ASW and PHU stations and (b) cross-wavelet spectrum between ASW and SJG stations.

magnetic parameters are the effects of the shock associated with the coronal mass ejection of 3 April 2010 which reaches the Earth on 5 April 2010 [*Möstl et al.*, 2010]. This CME is followed by high-speed solar wind streams related to coronal hole as shown in Figure 2 and Table 4; the effects of the coronal hole are observed on the days after the shock. On the first day, 5 April, all the stations exhibit similar and simultaneous signature of the prompt penetration of the convection electric field strongly at the European-African sector. On the days after 5 April, on 6–8 April, the disturbance is different from one station to another station. This fact indicates that the disturbance is not due to prompt penetration of the convection electric field. In Figures 4–6 the DP2 equivalent current due to the prompt penetration of magnetospheric convection is large during the phases of the storm period. Many short fluctuations of D_{iono} were observed and can be attributed to the DP2. In Figures 7–9, we observe on 5–7 April, three main minima of D_{iono} at daytime which are the signature ionospheric disturbance dynamo in agreement with model [*Blanc and Richmond*, 1980]. We observe also a smaller minimum on 8 April. The disturbance D_{iono} main pattern is related to the DP2 current system [*Nishida*, 1968] and D_{dyn} current system [*Le Huy and Amory-Mazaudier*, 2005]. We separate the effect of DP2 from the disturbance dynamo in Figure 10 in order to analyze the sole effect of the ionospheric disturbance dynamo. We average value of 4 h of D_{iono} data with sliding of 1 h for the whole period of study for ASW, PHU, and SJG stations by using some MATLAB programs (interpolation, average, and mean). Table 5 gives the LT time of the maxima of Ddyn.

We used continuous wavelet transformation showing that the dominant period of the D_{dyn} which is characterized by high power spectrum in the period with an average value of

22 h in Figures 11 and 12. The cross-wavelet spectrum analysis revealed that the D_{dyn} has a direction from PHU passing by ASW then to SJG or from west to east direction.

4. Results and Discussion

The CME impacted the Earth's magnetosphere on 5 April 2010 at SSC 08:25 UT during the beginning of the main phase of the storm (see Figure 2), from 08:25 UT to 14:00 UT, the *Vx* increased suddenly (500–800 km/s), also *Bz* changed from southward to northward and southward again. The *AU* and *AL* exhibited maxima (500 nT and −2000 nT). The ground magnetic observations associated to the changes in *Bz AU* and *AL* can be interpreted as the effect of the prompt penetration of magnetospheric convection electric field [*Vasyliunas*, 1970]. Indeed, this physical process affects simultaneously high, middle, low, and equatorial latitudes. When *Bz* is northward at 12:00 UT, we observe a strongest decrease of *H* component at African sector, see Figures 4a, 5a, and 6a. But at that time another physical process, the ionospheric disturbance dynamo [*Blanc and Richmond*, 1980] can also be invoked to explain the observations. We observe also that several hours is the time delay needed by the ionospheric disturbance dynamo to reach low latitudes, where the neutral winds play an important role at low latitude after several hours [*Fejer et al.*, 1983; *Sastri*, 1988; *Yigenzaw et al.*, 2005]. The eastward prompt penetration electric field associated with the southward IMF *Bz* at around 13:30 UT increases the regular daytime eastward dynamo electric field. On 6 April 2010, there is long time duration of southward *Bz* (Figure 2b), and strong westward electrojet (Figure 2d). During the recovery phase we observe always the same feature, three minima of D_{iono} (Figures 6–8) on 6–8 April 2010. This is the signature of the ionospheric disturbance dynamo [*Blanc and Richmond*, 1980] which causes at low latitudes a reverse *Sq* current system. The perturbation of D_{iono} main pattern is related to DP2 current system [*Nishida*, 1968] and Ddyn current system [*Le Huy and Amory-Mazaudier*, 2005]. We can see the superposition of DP2 current (fluctuations of signal of few hours) and Ddyn (strong minimum of the signal around daytimes). It is the first time that we separate the effect of Ddyn from the DP2 current system and therefore observe at several latitudes during several days the sole effect of the ionospheric disturbance dynamo associated to high-speed solar wind streams. The ionospheric disturbance dynamo process was previously analyzed by several authors particularly during super storms of October 2003 [*Sahai et al.*, 2005; *Abdu et al.*, 2007]. But super storms are produced by CME event with shocks which are not, in general, followed by high-speed solar wind streams as it is the case in the present study. The long duration of the Ddyn disturbance (several days) observed for this case study is related to the existence of the high-speed solar wind streams during several days. The strong enhancement in the *H* component at the magnetic equator observed for the AAE stations is due to the fact that the strongest disturbance occurred when AAE is on the dayside.

Global analyses of geomagnetic disturbances like these have been presented by *Price and Wilkins* [1963], *Price and Stone* [1964], *Matshushita* [1967, 1968], *Parkinson* [1971], *Malin* [1973], *Suzuki* [1973, 1978], *Main and Gupta* [1977], and *Winch* [1981].

At the northern crest stations (ASW, PHU, and SJG), Figure 10 illustrates the different responses of ionospheric disturbance dynamo in the different longitude sectors with the strongest response at African sector under the influence of a high-speed streams during 4 days. Finally, the wavelet analysis (Figures 10 and 11) illustrates very clearly the characteristics of Ddyn signal.

5. Conclusion

In this paper we analyzed the magnetic disturbance associated to the storm of 5 April 2010. This storm was initiated by a CME impacting the Earth on 5 April at 08:25 UT. On 6–8 April 2010, the CME was followed by high-speed solar wind streams associated to a coronal hole. We concentrate our study on the ionospheric part of this disturbance D_{iono}. We propose a method to analyze the part of Ddyn (part of D_{iono}) associated to the storm neutral winds created by auroral Joule heating.

1. During the initial phase of the storm, several hours after the SSC, on 5 April, we observe at low latitudes a first minima of the D_{iono} in Figures 7–9 which is related to the ionospheric disturbance dynamo which reverses the *Sq* current system in agreement with ionospheric disturbance dynamo model [*Blanc and Richmond*, 1980].
2. During the recovery phase we observe always the same feature; three minima of D_{iono} appear at daytime in Figures 7–9 on 6–8 April. These are signature of the ionospheric disturbance dynamo.

3. The disturbance D_{iono} main pattern is related to the DP2 current system [*Nishida*, 1968] and Ddyn current system [*Le Huy and Amory-Mazaudier*, 2005], so we separate the effect of DP2 from the disturbance dynamo in Figure 10, in order to analyze the sole effect of the ionospheric disturbance dynamo.
4. The ionospheric disturbance dynamo effect is observed on Ddyn during several days (days of high-speed solar wind streams) with amplitude decreasing with time. This disturbance depends on local time (see Table 5).
5. The strongest effect Ddyn is observed in the European-African longitude sector due to the local time location at the time of SSC onset.
6. The wavelet analyses show that the period of Ddyn is 22 h (approximately diurnal).
7. The cross-wavelet analysis confirms that the Ddyn is first observed at PHU, then at ASW and after at SJG.

Le Huy and Amory-Mazaudier analyzed Ddyn on specific days without DP2 current system extending from high to low latitudes. In the present case we analyze the sole Ddyn signature for days with DP2 current system. We eliminate the effects of the DP2 current system by taking into account its time variations (1–3 h). This is a new step in the study of Ddyn.

In this paper we analyzed the magnetic field variations associated with two main large-scale mechanisms of coupling between high and low latitudes: (1) the mechanism of prompt penetration of magnetospheric convection associated with the magnetic variation DP2 [*Nishida*, 1968] and (2) the mechanism of the ionospheric disturbance dynamo associated disturbed with the magnetic variation Ddyn [*Le Huy and Amory-Mazaudier*, 2005]. The originality of the work is to treat the signal in order to separate the two contributions that do not have the same temporal and spatial characteristics.

It is well known that the vertical E × B velocity at the equator plays a dominant role on the equatorial electrodynamics. Unfortunately, there are no direct measurements of the electric field in the African sector as it is the case in the American sector with the Jicamarca radar. A method based on the use of magnetic data to estimate the vertical velocity E × B was developed by *Anderson et al.* [2004]. In their study, Anderson et al. used two magnetic stations located at the same longitude and separated by few degrees in latitude. One station was located at the equator and the other in a region between 6 and 9° of the equator. This method was used by *Anderson et al.* [2002] for American sector (Peru) and Asian sector (Philippines and India). Unfortunately, this work was not possible to do the same for the African sector, this being due to the lack of magnetic stations.

A theoretical work done by *Fang et al.* [2008] used the TIEGCM model to estimate the magnetic effects related to ionospheric disturbance dynamo which is different from that associated with the prompt penetration of magnetospheric convection electric field. This work shows that before 12:00 LT the magnetic disturbance of the ΔH component due to the ionospheric disturbance dynamo is negative and then positive. We observe such a negative effect on H component in Figure 10 followed by an increase. *Fang et al.* [2008] also showed that there is a linear relationship between the variation of the magnetic field and ΔH and the E × B vertical velocity. This feature is observed by the Jicamarca radar during this event (http://jro.igp.gob.pe/driftnn/).

In conclusion, it is important to deploy instruments in Africa, such as incoherent scatter sounder in order to understand the whole world signature of the magnetic disturbances and the electrodynamics of the ionosphere at the origin of these disturbances.

Acknowledgments
My sincere thanks to all members of the Space Weather Monitoring Center, SWMC, Helwan University, for their ceaseless support. The CFCC-PhD program is financially supported by the French-Egypt scientific year project that cooperates with the Department of Scientific and Technological Cooperation Embassy of France in the Arab Republic of Egypt, French Institute of Egypt, and LPP/Polytechnique/UPMC/CNRS. Magnetometers were deployed in Egypt under the ISWI (International Space Weather Initiative) project which follows the IHY (International Heliophysical Year) project. Our warmest thanks go to the great efforts of the coordinators from all organizations (SWMC, Helwan University, CFCC, French-Egypt scientific year project, LPP/Polytechnique/UPMC/CNRS, ISWI, and IHY). The authors thank the INTERMAGNET project who contributed to the collection and data processing during the research. We would like to appreciate the powerful free wavelet software built by *Grinsted et al.* [2004] available on http://noc.ac.uk/using-science/crosswavelet-wavelet-coherence, which added a significant proof for the propagation of the Ddyn in this paper. The authors thank Paul Vila for the correction of English.

Robert Lysak thanks Mark Moldwin and two anonymous reviewers for their assistance in evaluating this paper.

References

Abdu, M. A., T. Maruyama, I. Batista, S. Saito, and M. Nakamura (2007), Ionospheric responses to the October 2003 superstorm: Longitude/local time effects over equatorial low and middle latitudes, *J. Geophys. Res.*, *112*, A10306, doi:10.1029/2006JA012228.

Anderson, D., A. Anghel, J. Chau, and O. Veliz (2004), Daytime vertical E × B drift velocities inferred from ground-based magnetometer observations at low latitudes, *Space Weather*, *2*, S11001, doi:10.1029/2004SW000095.

Anderson, D., A. Anghel, K. Yumoto, M. Ishitsuka, and E. Kudeki (2002), Estimating daytime vertical E × B drift velocities in the equatorial F-region using ground-based magnetometer observations, *Geophys. Res. Lett.*, *29*(12), 1596, doi:10.1029/2001GL014562.

Blanc, M., and A. D. Richmond (1980), The ionospheric disturbance dynamo, *J. Geophys.*, *85*(A4), 1669–1686, doi:10.1029/JA85iA04p01669.

Cole, K. D. (1966), *Magnetic Storms and Associated Phenomena*, *Space Science Reviews*, vol. 5, pp. 699–770, D. reidel publishing Company, Dordrecht, Netherlands.

Connors, M., C. T. Russell, and V. Angelopoulos (2011), Magnetic flux transfer in the 5 April 2010 Galaxy 15 substorm: An unprecedented observation, *Ann. Geophys.*, *29*, 616–622, doi:10.5194/angeo-29-619-2011.

Grinsted, A., J. C. Moore, and S. Jevrejeva (2004), Application of the cross wavelet transform and wavelet coherence to geophysical time series, *Nonlinear Processes Geophys.*, *11*(5/6), 561–566.

Fambitakoye, O., M. Menvielle, and C. Mazaudier (1990), Global disturbance of the transient magnetic field associated with thermospheric storm winds on March 23, 1979, *J. Geophys. Res.*, *95*, 15,209–15,218, doi:10.1029/JA095iA09p15209.
Fang, T. W., A. D. Richmond, J. Y. Liu, and A. Maute (2008), Wind dynamo effects on ground magnetic perturbations and vertical drifts, *J. Geophys. Res.*, *113*, A11313, doi:10.1029/2008JA013513.
Fejer, B. G., M. F. Larsen, and D. T. Farley (1983), Equatorial disturbance dynamo electric fields, *Geophys. Res. Lett.*, *10*, 537–540, doi:10.1029/GL010i007p00537.
Fukushima, N., and Y. Kamide (1993), Partial ring current models for worldwide geomagnetic disturbances, *Rev. Geophys. Space Phys.*, *11*(4), 795–873.
Huang, C. M. (2013), Disturbance dynamo electric field in response to geomagnetic storms occurring at different universal times, *J. Geophys. Space Physics*, *118*, 496–501, doi:10.1029/2012JA018118.
Le Huy, M., and C. Amory-Mazaudier (2005), Magnetic signature of the ionospheric disturbance dynamo at equatorial latitudes: "Ddyn", *J. Geophys. Res.*, *110*, A10301 doi:10.1029/2004JA010578.
Le Huy, M., and C. Amory-Mazaudier (2008), Planetary magnetic signature of the storm wind disturbance dynamo currents: Ddyn, *J. Geophys. Res.*, *113*, A02312, doi:10.1029/2007JA012686.
Main, S. R. C., and J. C. Gupta (1977), The Sq current system during the International Geophysical Year, *Geophys. J. R. Astron. Soc.*, *49*, 515.
Malin, S. R. C. (1973), Worldwide distribution of geomagnetic tides, *Philos. Trans. Soc. London*, *A274*, 551.
Matshushita, S. (1967), Solar quiet and lunar daily variations fields, in *Physics of Geomagnetic Phenomena*, edited by S. Matshushita and W. H. Campbell, 301 pp., Academic Press, New York.
Matshushita, S. (1968), Sq and L current system in the ionosphere, *Geophys. J. R. Astron. Soc.*, *15*, 109.
Mayaud, P. N. (1980), *Derivation, Meaning and Use of Geomagnetic Indices*, *Geophys. Monogr. Ser.*, vol. 22, 154 pp., AGU, Washington, D. C.
Mayaud, P. N. (1982), Comment on "The ionospheric disturbance dynamo" by Blanc and A. D. Richmond, *J. Geophys. Res.*, *87*, 6353–6355, doi:10.1029/JA087iA08p06353.
Mazaudier, C., and S. V. Venkateswaran (1990), Delayed ionospheric effects of geomagnetic storms on March 22, 1979 studied by the sixth Coordinated Data Analysis Workshop (CDAW-6), *Ann. Geophys.*, *8*, 511–518.
Menvielle, M., and A. Marchaudon (2008), Geomagnetic indices, in *Solar-Terrestrial Physics and Space Weather in Space Weather*, edited by J. Lilensten, pp. 277–88, Springer, Netherlands.
Möstl, C., M. Temmer, T. Rollett, C. J. Farrugia, Y. Liu, A. M. Veronig, M. Leitner, A. B. Galvin, and H. K. Biernat (2010), STEREO and Wind observations of a fast ICME flank triggering a prolonged geomagnetic storm on 5–7 April 2010, *Geophys. Res. Lett.*, *37*, L24103, doi:10.1029/2010GL045175.
Nishida, A. (1968), Geomagnetic DP2 fluctuations and associated phenomena, *J. Geophys. Res.*, *73*, 1795–1803, doi:10.1029/JA073i005p01795.
Nishida, A., N. Iwasaki, and N. T. Nagata (1966), The origin of fluctuations in the equatorial electrojet: A new type of geomagnetic variation, *Ann. Geophys.*, *22*, 478–484.
Parkinson, W. D. (1971), An analysis of the geomagnetic diurnal variation during the international geophysical year, *Gerlands Beitr. Geophys.*, *80*, 199.
Price, A. T., and D. J. Stone (1964), The quit-day magnetic variations during IGY, *Ann. IGY*, *35*, 63.
Price, A. T., and G. A. Wilkins (1963), New methods for the analysis of geomagnetic fields and their application to Sq field pf 1932–1933, *Philos. Trans. R. Soc.*, *A256*, 31.
Richmond, A. D., C. Peymirat, and R. G. Roble (2003), Lon-lasting disturbances in the equatorial ionospheric electric field simulated with a coupled magnetosphere-ionosphere-thermosphere model, *J. Geophys. Res.*, *108*(A2), 1118, doi:10.1029/2002JA009493.
Sahai, Y., et al. (2005), Effects of the major storms of October 2003 on the equatorial and low-latitude F region in two longitudinal sectors, *J. Geophys. Res.*, *110*, A12591, doi:10.1029/2004JA010999.
Sastri, H. (1988), Equatorial electric field of ionospheric disturbance dynamo origin, *Ann. Geophys.*, *6*, 635–642.
Shimeis, A., I. Fathy, C. Amory-Mazaudier, R. Fleury, A. M. Mahrous, A. Yoshikawa, and K. Groves (2012), Signature of the coronal near the north crest equatorial anomaly over Egypt during the strong geomagnetic storm 5 April 2010, *J. Geophys. Res.*, *117*, A07309, doi:10.1029/2012JA017753.
Suzuki, A. (1973), A new analysis of the geomagnetic Sq field, *J. Geomagne. Geoelectr.*, *25*, 259.
Suzuki, A. (1978), Geomagnetic Sq field at successive universal times, *J. Atmos. Sol. Terr. Phys.*, *40*, 449.
Vasyliunas, V. M. (1970), Mathematical models of the magnetospheric convection and its coupling to the ionosphere, in *Particles and Fields in the Magnetosphere*, edited by M. mcCormac, pp. 60-71, Springer, New-York, doi:10.1007/978-94-010-3284-1-6.
Winch, D. E. (1981), Spherical harmonic analyses of geomagnetic tides 1964–1965, *Philos. R. Soc.*, *A303*, 1.
Yigenzaw, E., P. L. Dyson, E. A. Essex, and M. D. Moldwin (2005), Ionospheric dynamics over the Southern Hemisphere during the 31 March 2001 severe magnetic storm using multi-instrument measurement data, *Ann. Geophys.*, *23*, 707–721, doi:10.5194/angeo-23-707-2005.
Zaka, K. Z., A. T. Kobea, P. Assamoi, O. K. Obrou, V. Doumbia, K. Boka, B. P. J. Adohi, and N. M. Mene (2009), Latitudinal profile of the ionospheric disturbance dynamo magnetic signature comparison with DP2 magnetic disturbance, *Ann. Geophys.*, *27*, 3523–3536.
Zaka, K. Z., et al. (2010), Simulation of electric field and current during the 11 June 1993 disturbance dynamo event: Comparison with the observations, *J. Geophys. Res.*, *115*, A12314, doi:10.1029/2010JA016292.